Service, Fatigue, and Ultimate Load Evaluation of a Continuous Prestressed Flat-Slab Bridge System

RONALD A. COOK, FERNANDO E. FAGUNDO, ADRIAN D. ROZEN, AND HASKEL MAYER

A new type of short-span bridge system for traversing wetlands and shallow waters (i.e., a trestle-type bridge) has been developed and implemented over the Albemarle Sound south of Edenton, North Carolina. The new system incorporates precast flat-slab sections that are posttensioned for continuity. The new system has the potential to replace traditional trestle-type bridges constructed using simple-span prestressed beams with a cast-in-place deck. A continuous two-span, half-scale model of this precast, posttensioned, flat-slab bridge system was built and tested under various load conditions. The bridge was evaluated analytically and experimentally for the transfer load case (deal load plus prestress), the maximum negative moment service load case, the maximum positive moment service load case, fatigue load, cracking load, and ultimate load. The model bridge performed as predicted for all load cases. Comparisons between analytical and physical models showed good correlation for all types of tests. At service load levels the bridge exhibited an elastic response with no evidence of cracking. The results of the fatigue load tests showed no degradation of stiffness. The ultimate load and deflections of the new bridge system were readily predicted by standard behavioral models for prestressed concrete. With the cost savings, short erection time, and multispan continuity of this system, it should be considered a viable alternative to the standard girder systems available for trestle-type bridges.

The selection of a bridge system for any application is linked to the site's physical constraints, such as clearances, accessibility, sensitivity of environment, location, and availability of local materials and labor. Even with these constraints a number of options remain to the designer, with the final selection usually directed by cost and aesthetics.

Much work has been done in the area of standard prestressed girders with cast-in-place bridge decks. These systems are currently being used with a high degree of efficiency. To realize further savings, new systems must be explored.

One new system consisting of a precast segmental flat-slab bridge, posttensioned for continuity, has the potential to replace most low, short-span bridges such as those that traverse wetlands and relatively shallow waters. This system has been used successfully over the Albemarle Sound south of Edenton, North Carolina (see Figure 1). A 50 percent to 60 percent cost savings could be obtained with this system for certain applications. The bid price for the superstructure of the existing bridge system was only $23/ft^2 (*1*).

R. A. Cook and F. E. Fagundo, Department of Civil Engineering, University of Florida, Gainesville, Fla. 32611. A. D. Rozen, Kimley-Horn & Associates, Inc., West Palm Beach, Fla. 33407. H. Mayer, E. N. Bechamps & Associates, Inc., Miami, Fla. 33126.

The cost savings is realized through an efficiently designed cross section and decreased labor costs through assembly-line production of individual segments. Another advantage of this system is an integrally cast pile cap in the bent segment. This allows for the segment to be placed directly on piles without the need for a bent to be formed and cast in the field. As with any standardized system, the savings are proportional to the repetition of the application.

OBJECTIVES

An experimental and analytical research program was undertaken to evaluate the behavior of the new bridge system.

The objectives of the research program were to

1. Develop and construct a physical scale model of the bridge system;
2. Test the model bridge system for service, fatigue, and ultimate loads;
3. Develop analytical models to predict the performance of the system; and
4. Verify the analytical results by comparing them with those obtained from experimental data to develop a degree of confidence in the new system.

EXISTING STRUCTURE

As mentioned, the original structure used as the basis for this study is a bridge over the Albemarle Sound in northeastern North Carolina on State Highway 32. The concept and design for the bridge were developed by the Figg Engineering Group. This posttensioned flat-slab concrete bridge system consists of precast segments that range from 4.57 to 6.10 m (15 to 20 ft) in length with a cross section 34 ft 3 in. 10.44 m wide and a center slap thickness of 413 mm (16¼ in.). The crown slope is 2 percent and the edge slab thickness is 203 mm (8 in.). The segments were transversely prestressed with both pretensioned and postensioned steel in the casting yard. The bridge was designed for three lanes of AASHTO (*2*) loading. The segments were placed on temporary steel erection girders that spanned pile groups (three piles per group). Concrete then was placed in 1-ft closure joints between each segment and in voids shaped like truncated pyramids directly over each

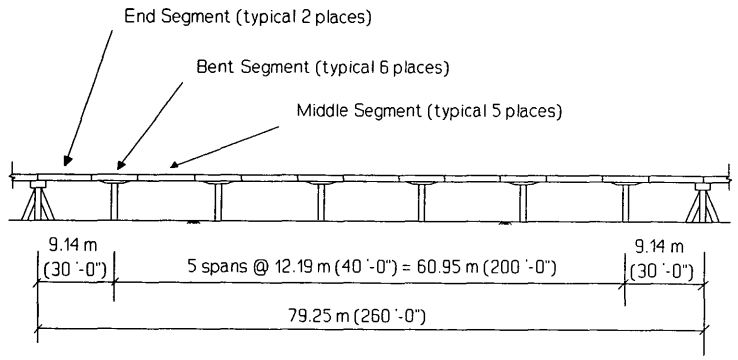

FIGURE 1 Existing bridge.

pile to create the section 79.25 m (260 ft) long shown in Figure 1. The section was posttensioned longitudinally, after which the temporary erection girders were removed. All posttensioning tendons were grouted. The total length of the original project was approximately 5.6 km (3.5 mi).

TEST SPECIMEN

When a new structural system is developed, it is important that the analytical models used to predict the behavior of the system be reliable. One method of ensuring the validity and reliability of the analytical models is by the physical testing of a scale model of the system. The results of the analytical models can then be compared with test results. The structural model chosen for this study is shown in Figures 2 and 3. The test specimen chosen represents a two-span, three-segment, half-scale model of the existing structure.

The model was constructed using two end segments and one bent segment from the existing structure (see Figure 1). Although the distance between the centerlines of the pile groups at the end spans was 9.14 m (30 ft), the actual span length was 8.79 m (28 ft 10 in.) because of end-bearing details. The span length of the model was exactly half that of the end spans of the existing structure as indicated in Figure 3. The actual length of the end segments in the model was slightly less than half the length of the full-scale end segment. The discrepancy results from a protective concrete cover that was provided over the tendon anchors in the existing structure.

All requirements for similitude between the model and existing system were met (*3*). To correctly model dead load, dead load compensating blocks were distributed evenly over the surface of the model bridge before posttensioning.

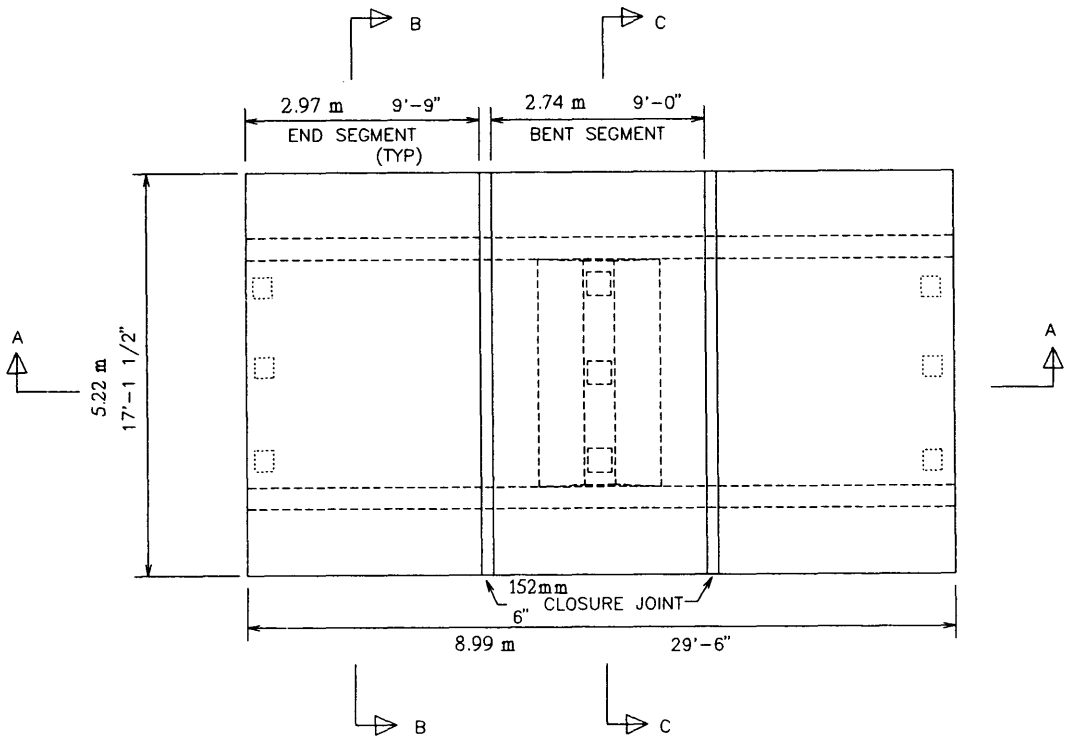

FIGURE 2 Model bridge: plan view.

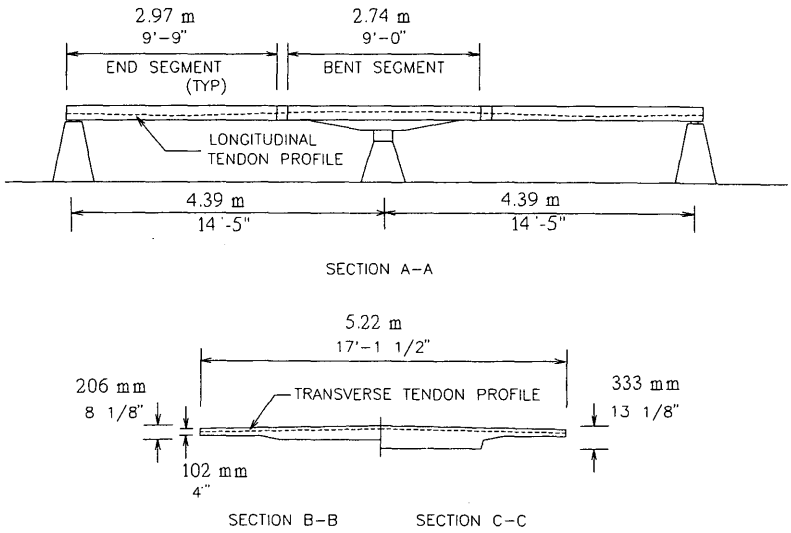

FIGURE 3 Model bridge: sections.

The model bridge was constructed using the same type of erection procedure as used for the existing structure. The bridge segments were cast on the floor of the laboratory. After curing, the segments were placed on temporary shoring located between the two end supports and center pier support shown in Figure 3. Closure pours were then made between the segments and in the three voids over the piers at the center support. The bridge was then posttensioned and the tendons were grouted, after which the temporary supports were removed.

All nonprestressed and prestressed reinforcement in the existing bridge system was duplicated in the model bridge with appropriate similitude requirements. The prestressing forces and losses were determined on the basis of the dimensions of the model bridge. Details of nonprestressed and prestressed reinforcement are provided by G. M Sabnis et al. (*3*). In the model, all prestressing strands were 13 mm (0.5 in.) in diameter, seven-wire, low-relaxation Grade 1860 MPa (270 ksi).

The concrete had a 28-day compressive strength of 37.9 MPa (5,500 psi). Displacements were measured with 20 linear variable differential transformers (LVDTs). Strains were measured with internal and surface strain gauges.

TEST SETUP

Three loading systems were used during the testing program. As shown in Figure 4, the service load tests (both static and fatigue) were performed using a test apparatus that reproduced the effects of three lanes of the AASHTO (*2*) HS20-44 truck load. Loading configurations were used that produced maximum positive and negative moments in the two-span continuous bridge. These loading configurations repre-

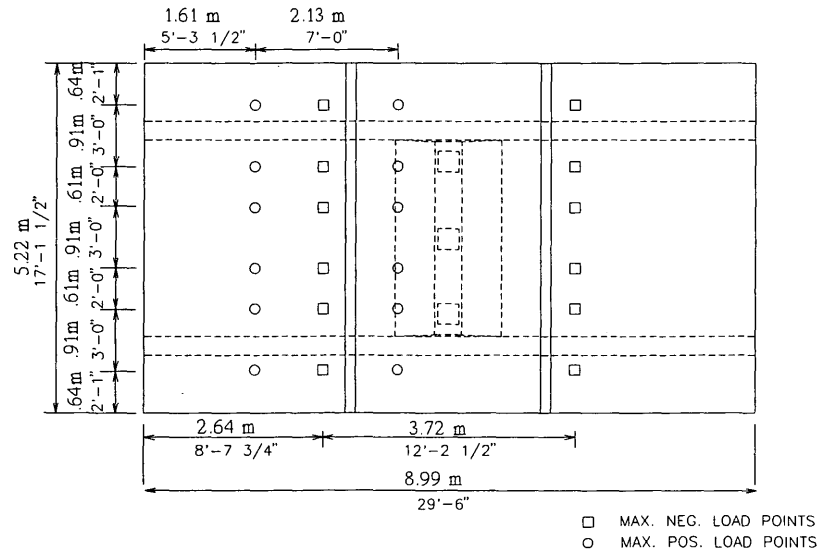

FIGURE 4 Load points for service load tests (static and fatigue).

sent the controlling design conditions for the existing bridge. Note that the loading arrangement shown in Figure 4 indicates only four wheel loads per truck. The effects of the front wheels of the standard AASHTO HS20-44 truck were neglected because their contribution to the overall maximum moment was insignificant. As shown in Figure 4, in the maximum positive moment test configuration all axle loads were placed in one span, whereas in the maximum negative moment test configuration the axle loads straddled the center support. To be sure of having equal loads on all wheels, the test rig was designed to be fully determinate by using a series of stacked beams and one central hydraulic ram.

A single line of concentrated loads was used for fatigue-load testing after cracking and for the ultimate load test. The loading arrangement used for these test series is shown in Figure 5. Analysis based on conventional prestressed, reinforced concrete beam theory indicated that the positive moment load case (i.e., all the load on one span) would control both the minimum cracking load and the ultimate load.

Because different loading configurations were used for the positive moment load case, it was necessary to establish the load equivalence between the configurations. For the three lanes of truck loading used in the service-level load tests (Figure 4), the maximum load applied to the system was 250 kN (56.2 kips). This load was based on three trucks, each with four wheel loads of 71 kN (16 kip). The AASHTO (*2*) multiplication factor of 1.30 for impact and 0.90 for three lanes of loading as well as the model scale factor of one-fourth for load were included in the calculation of this load. For the single line load configuration used for the ultimate load tests, the equivalent load was determined to be 147 kN (33.0 kips). The equivalence of this load was determined analytically by influence lines and verified experimentally by both strain and deflection measurements. This means that a total load of 147 kN (33.0 kips) applied as shown in Figure 5 produced the same maximum strain and deflection as a total load of 250 kN (56.2 kips) applied in the positive moment load configuration shown in Figure 4. Therefore, a 1.70 multiplication factor should be used to determine the equivalent Figure 4 load for a load applied in the Figure 5 test setup.

SERVICE LOAD TESTS

Experimental results obtained from the transfer (dead load plus prestress) load case, the maximum positive moment service load case, and the maximum negative moment service load case are discussed and compared to analytical results. Analytical results were obtained from a finite element analysis (FEA) of the prestressed bridge system performed with commercially available software (*4*).

Unless noted, all experimental results represent only the load case under consideration (i.e., transfer plus dead load, live load positive moment, and live load negative moment). For example, the deflections shown for the positive moment load case are the deflections that occurred during that load case only, not the total deflections that occurred since construction of the model. For the figures in this paper, positive deflection is defined as up.

Test Results for Transfer (Dead Load plus Prestress)

Figure 6 shows the deflection profile measured along the longitudinal centerline axis of the bridge. In Figure 6, the experimental data in general show the same shape as the analytical data. One span exhibited higher experimental deflections and the other span exhibited lower deflections compared to the analytical solution. As more of the longitudinal stressing occurred from the end with the higher deflections, this appears to be reasonable. The loss of prestress because of tendon friction and wobble would cause the deflections for the span farthest from the stressing operation to have lower deflections.

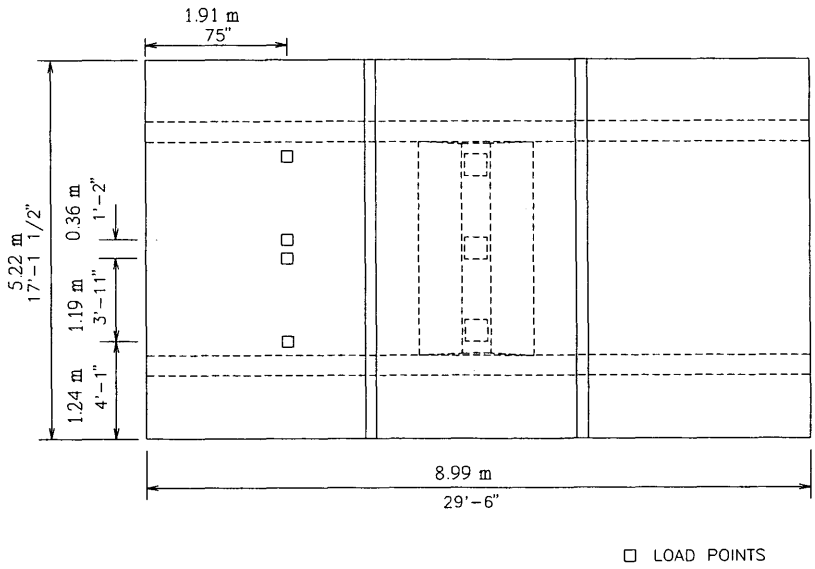

FIGURE 5 Load points for cracking, fatigue load after cracking, and ultimate load tests.

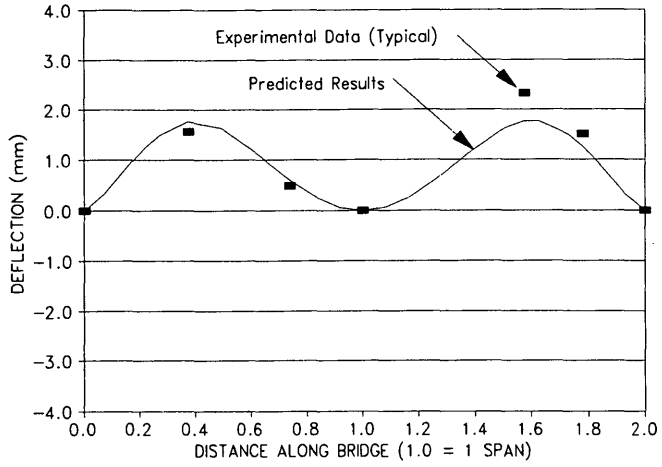

FIGURE 6 Longitudinal deflection for transfer (dead load and prestress).

Results for Maximum Positive Moment Service Load Test

Figure 7 presents the longitudinal deflection curve at the centerline of the bridge for the positive moment load case. The shape of the longitudinal profile appears to indicate that the structure was not performing as expected. Although the basic form of the deformations is close to that predicted, the magnitude of the measured deflections is smaller than those obtained from the analysis. In the analysis, the center support was modeled as a frictionless hinge whereas the end supports were modeled as rollers. The test indicates that some stiffness was in fact associated with the center pile support constructed in the laboratory that allowed less rotation than expected; this stiffness accounts for the differences in deflections. The pile support constructed in the laboratory incorporated a built-in hinge 229 mm (9 in.) below the bottom of the bridge deck (5).

Test results for load-strain and load-deflection relationships at all locations indicated linear response. Stress distributions through the slab thickness (determined from strain measurements at the top, interior, and bottom of the slab) indicated linear distribution in close agreement with analytical results.

Results for Maximum Negative Moment Service Load Test

The longitudinal deflection profile in Figure 8 shows very good correlation between experimental and predicted results. The right span's deflections were slightly less than those predicted. This is attributed to that span having a greater prestress force, which would tend to reduce deflections due to live load. Load-strain and load-deflection relationships at all locations indicated a linear elastic response.

Discussion of Service Load Test Results

The experimental results closely matched those predicted by the analysis for all individual load cases. As previously noted, the major differences occurred in the cases of transfer and maximum positive moment load. For the case of maximum negative moment load, the experimental and analytical results matched almost exactly.

In the transfer load case, the measured deflections were slightly higher than predicted in one span and lower than predicted in the other. This difference can be attributed to the posttensioning sequence used in construction of the bridge.

In the maximum positive moment load case, the measured deflections were slightly less than expected in both spans. This result can be attributed to the rotational stiffness of the center pier support, which was not accounted for in the analysis. The rotational stiffness of this support reduced the moment transfer between spans. The result was smaller experimental deflections than predicted by the analysis.

In summary, the model bridge performed very well and remained in the elastic range of behavior. The test results were close to the analytical predictions for each load case. The service load tests are discussed further elsewhere (5).

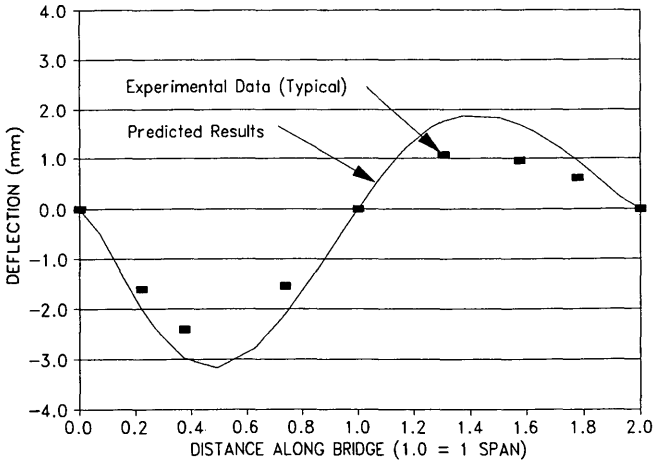

FIGURE 7 Longitudinal deflection for maximum positive moment service load test.

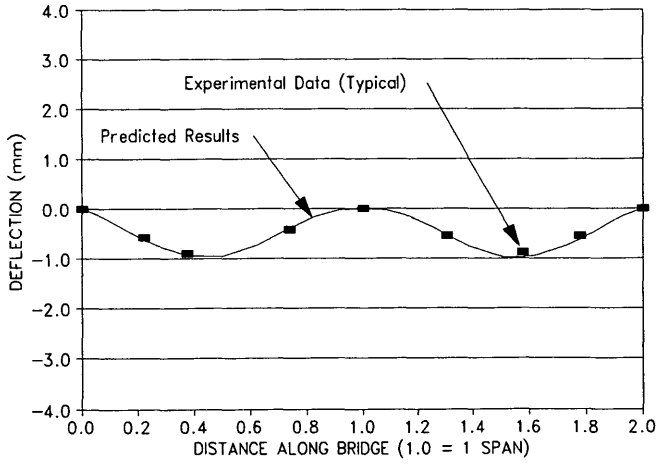

FIGURE 8 Longitudinal deflection for maximum negative moment service load test.

FATIGUE LOAD TESTS

Two types of fatigue load tests were performed. The first type of fatigue load test was performed for the maximum service level fatigue loading expected on the bridge. This maximum was considered to be two lanes of AASHTO HS20-44 truck loading. This condition assumes that two trucks are located at the worst possible position at the same time. This type of fatigue test was conducted for a total of 3 million cycles, which was considered to be far in excess of the number of cycles that the actual bridge would experience for this load condition. The loading was applied as shown in Figure 4. The total load for this type of test was determined to be 185 kN (41.6 kips) based on eight wheel loads of 71 kN (16 kips), an impact factor of 1.3, and a model scale factor of one-fourth for load.

The second type of fatigue load test was conducted after the bridge was cracked. The loading configuration shown in Figure 5 was used for this test. The maximum fatigue load for this type of test was 150 percent of the design service load of three lanes of AASHTO HS20-44 truck loading. Two million cycles of fatigue load were performed for this type of test.

To determine if any degradation in stiffness had occurred, a static load test equivalent to the maximum service level design load of three AASHTO HS20-44 trucks was performed about every 100,000 cycles. For each of these static tests, the relative stiffness of the system was evaluated by dividing the applied load by the displacement measured at different locations in the spans.

Results for Fatigue Load Tests

Two load configurations were used for the service level fatigue load tests. The first 2 million cycles of load were applied with the test setup in the maximum negative moment test configuration (see Figure 4). Another 1 million cycles of loading were performed with the test setup in the test configuration of maximum positive moment (see Figure 4). Figure 9 shows the actual load history for these tests as a percent of the two-lane AASHTO HS20-44 truck loading. No degradation in stiffness or variation from linear behavior was observed during these tests.

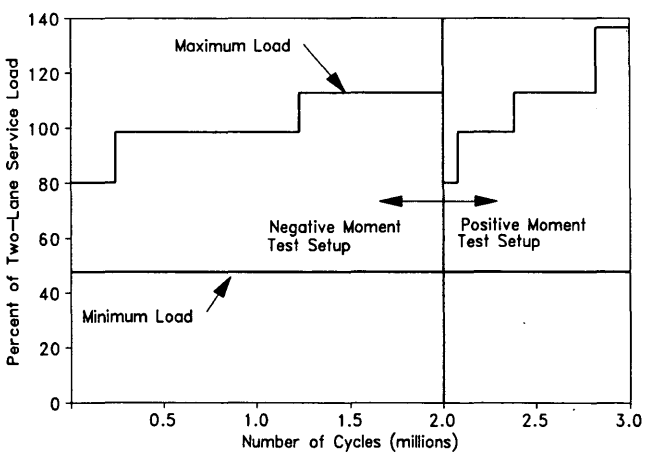

FIGURE 9 Load history for service level fatigue tests.

After the service-level fatigue load tests were performed, the loading configuration was changed to the single line loading indicated in Figure 5. The bridge was then loaded monotonically until cracking occurred at a load of 418 kN (94 kips). As observed, this load was equivalent to 710 kN (160 kips) applied in the positive moment test configuration in Figure 4 (1.70 multiplication factor for converting Figure 5 loads to Figure 4 loads). After the bridge was cracked, another 2 million cycles of load was applied in the test configuration in Figure 5. The maximum load applied for this test was 220 kN (49.5 kips) and the minimum load was 89 kN (20 kips). The maximum load was equivalent to 150 percent of the three-lane service load, 200 percent of the two-lane service load, 28 percent of the predicted ultimate load, and 26 percent of the measured ultimate load. No degradation of stiffness or variation in linear behavior was observed over the course of this test.

Discussion of Fatigue Load Test Results

No degradation of stiffness or structural integrity was noted during any of the fatigue load tests. The system response remained linear elastic throughout the fatigue load testing program. This is not surprising as the load applied in these tests was below the cracking load of the prestressed bridge system. As with most prestressed, posttensioned systems with grouted tendons, reasonable fatigue loading does not affect the integrity of the system. To obtain early fatigue failure, the bridge would need to be subjected to fatigue loads above cracking. In the case of this particular system, this would amount to a loading above 50 percent of the ultimate load or 270 percent of the three-lane design service load. Because these load levels will never be experienced in the actual bridge, it is reasonable to assume that fatigue loading is not a problem for the new bridge system. Further discussions of the fatigue load tests are presented elsewhere (*6,7*).

ULTIMATE LOAD TEST

The predicted behavior from service load to ultimate load was determined from conventional prestressed, reinforced concrete beam theory (*8*). The analysis indicated that the critical load condition was controlled by flexure due to positive moment. Punching shear at the center piers, negative moment over the piers, and negative moment in the unloaded span also were investigated as possible critical load conditions. These factors were found not to produce the minimum cracking or failure load on the bridge system.

For cracking and ultimate load analysis, the entire cross section of the three-lane bridge was considered a longitudinally spanning beam continuous over three supports. The moment-curvature diagrams for both the loaded and unloaded spans were developed to predict the results. Because the cross section and reinforcement in both spans were identical, one moment-curvature diagram was developed. The live load produces positive curvature in the loaded span, whereas in the unloaded span the live load produces negative curvature. The

moment-curvature diagrams for both spans are shown in Figure 10. Before the addition of any live load, the moment in both spans resulting from dead load and secondary moments was determined to be 55.6 kN-m (41 kip-ft). According to Figure 10, this indicates an initial negative curvature in both spans that is verified by Figure 6.

The values on the moment-curvature diagram in Figure 10 were used to predict the cracking load of 342 kN (77 kips) and ultimate load of 787 kN (177 kips) of the bridge system. The moment-curvature diagram in Figure 10 was also used to predict the load-strain and load-deflection behavior of the system.

Results for Ultimate Load Test

Figure 11 shows the measured longitudinal displacements for various stages of the ultimate load test. Displacements were linear up to the cracking load of 418 kN (94 kips). After initial cracking in the loaded span, the deflection under the load increased significantly. The unloaded span also cracked at the construction joint between segments before ultimate load and began to experience large upward deflections. The observed crack in the construction joint was minimal and confined to the interface between the cast-in-place closure joint and the end segment. The formation of this crack should not be considered to be detrimental to the performance of the bridge system because it occurred at a load substantially higher than the design service load.

Figure 12 shows the predicted and measured strains on the top surface of the concrete at the bridge centerline directly under the load for the ultimate load test. The predicted and measured strains are in close agreement. Figure 13 shows the measured load-deflection relationship at the bridge centerline directly under the load compared to the calculated load-deflection relationship for the ultimate load test. Figure 13 indicates that the predicted results are in close agreement with test results.

The actual ultimate load for the bridge system was 832 kN (187 kips). The controlling failure mode was by flexural failure

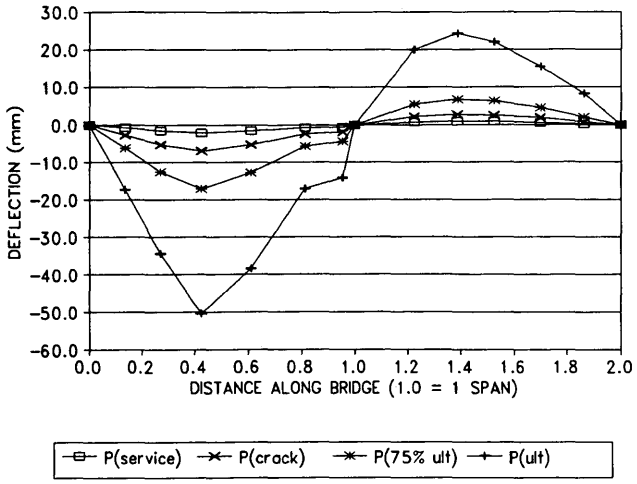

FIGURE 11 Longitudinal deflection for ultimate load test.

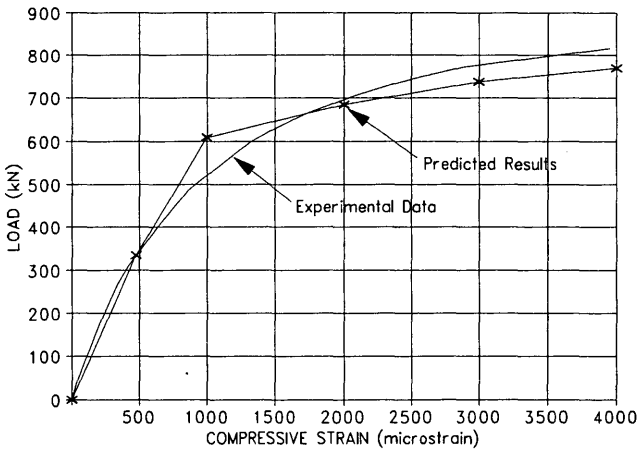

FIGURE 12 Maximum top surface compressive strains for ultimate load test.

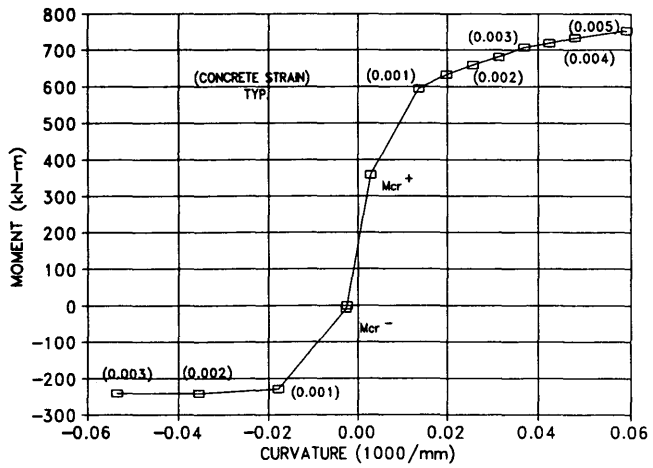

FIGURE 10 Moment-curvature diagram for loaded and unloaded spans.

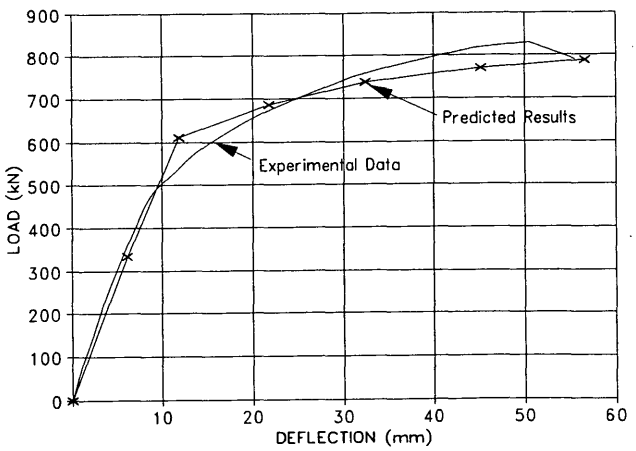

FIGURE 13 Load-deflection diagram for ultimate load test.

resulting from crushing of the concrete at the top surface of the bridge deck directly under the load. The flexural compression failure occurred over about half the width of the bridge at this location.

Discussion of Ultimate Load Test Results

Both Figures 12 and 13 show that the predicted results are in close agreement with test results. This fact indicates that the behavior of the bridge system from service load to cracking load and from cracking load to ultimate load is readily predictable by the theory of conventional prestressed, reinforced concrete beam. The ratio of experimental to predicted cracking load was 1.22, and the ratio of experimental to predicted ultimate load was 1.06.

In both experimental and predicted results, the cracking load was about 2.5 times the design service load, and the ultimate load was about 5.5 times the design service load. Further discussion of the ultimate load test is presented elsewhere (*7*).

SUMMARY

A half-scale model of a flat-slab bridge system that was continuous, precast, and posttensioned was built and tested for service load, fatigue load, and ultimate load. Individual load cases studied included transfer (dead load plus prestress), maximum negative service load moment, maximum positive service load moment, fatigue load before and after cracking, and ultimate load. Analytical models were developed and the results were compared to experimental results.

For the tests of service load, the model bridge remained in the linear elastic response range throughout its loading history. No cracking developed and the data indicated that the bridge remained in compression for all load cases. Test results compared well with results predicted by analysis.

No degradation of stiffness or loss of structural integrity was noted in 5 million cycles of fatigue loading. The behavior of the bridge system remained linear after the fatigue load tests.

The results of the ultimate load test indicate that the behavior of the bridge system can be determined from conventional prestressed, reinforced concrete beam theory. Both the cracking strength and ultimate strength of the system were well in excess of minimum AASHTO requirements.

CONCLUSIONS

The multispan bridge system appears to be an excellent alternative to the standard simple-span prestressed girder system for short-span applications that traverse wetlands and shallow water. The behavior of the new system is readily predicted by standard analytical and behavioral models.

With the apparent cost savings, short erection time, and multispan continuity of this system, it should certainly be considered as an alternative to the simple-span prestressed girder system with a cast-in-place deck for this application.

ACKNOWLEDGMENTS

The research reported in this paper was conducted in the Structures Laboratory at the University of Florida. This research was sponsored by the Florida Department of Transportation. The successful completion of this project would not have been possible without the contributions of materials, time, and technical expertise from the following manufacturers: Crom Corporation; Dywidag Systems International; Florida Rock Industries; Florida Wire and Cable Company; Owens Steel Company; Painter Masonry, Inc.; and Steel Fab, Inc.

REFERENCES

1. H. Carr and M. May. A Sound Investment: Trestle at $23 per Sq. Ft. *Engineering News Record*, Vol. 221, No. 8, Aug. 25, 1988, pp. 30–31.
2. *Standard Specifications for Highway Bridges: Interim Specifications—Bridges—1990*, 14th ed. AASHTO, Washington, D.C., 1990.
3. G. M. Sabnis, H. G. Harris, R. N. White, and M. S. Mirza. *Structural Modeling and Experimental Techniques*. Prentice-Hall, Inc., Englewood Cliffs, N.J., 1983.
4. E. L. Wilson and A. Habibullah. *SAP90: A Series of Computer Programs for the Static and Dynamic Finite Element Analysis of Structures*. Computers & Structures, Inc., Berkeley, Calif., 1989.
5. R. A. Cook, F. E. Fagundo, B. A. Munson, B. M. Schafer, and D. E. Richardson. *Analytical and Experimental Evaluation of a Precast, Post-Tensioned, Segmental Flat Slab Bridge System for Service Loads*. Structures and Materials Research Report No. 91-2, University of Florida, Gainesville.
6. H. Mayer. *Analytical and Experimental Evaluation of a Precast, Post-Tensioned, Segmental Flat Slab Bridge System for Service Level Fatigue Loading*. Master's thesis. Department of Civil Engineering, University of Florida, Gainesville, Aug. 1992.
7. A. D. Rozen. *Evaluation of a Post-Tensioned Flat Slab Bridge System for Fatigue and Ultimate Load*. Master's thesis. Department of Civil Engineering, University of Florida, Gainesville, Aug. 1992.
8. T. Y. Lin and N. H. Burns. *Design of Prestressed Concrete Structures, 3rd ed.* John Wiley & Sons, New York, N.Y., 1981.

Publication of this paper sponsored by Committee on Concrete Bridges.